

**Towards accounting
for dissolved iron
speciation**

A. Tagliabue and
C. Völker

Towards accounting for dissolved iron speciation in global ocean models

A. Tagliabue^{1,2,3} and **C. Völker**⁴

¹Laboratoire des Sciences du Climat et de l'Environnement, UMR 8212, IPSL-CEA-CNRS-UVSQ Orme des Merisiers, 91198 Gif sur Yvette, France

²Council for Scientific and Industrial Research, Natural Resources and the Environment, P.O. Box 320, Stellenbosch, 7599, South Africa

³Department of Oceanography, University of Cape Town, 7701 Cape Town, South Africa

⁴Alfred Wegener Institute for Polar and Marine Research, Am Handelshafen 12, 27570 Bremerhaven, Germany

Received: 9 February 2011 – Accepted: 26 February 2011 – Published: 16 March 2011

Correspondence to: A. Tagliabue (atagliab@gmail.com)

Published by Copernicus Publications on behalf of the European Geosciences Union.

Title Page

Abstract

Introduction

Conclusions

References

Tables

Figures

⏪

⏩

◀

▶

Back

Close

Full Screen / Esc

Printer-friendly Version

Interactive Discussion

Abstract

The trace metal iron (Fe) is now routinely included in state-of-the-art ocean general circulation and biogeochemistry models (OGCBMs) because of its key role as a limiting nutrient in regions of the world ocean important for carbon cycling and air-sea CO₂ exchange. However, the complexities of the seawater Fe cycle, which impact its speciation and bioavailability, are highly simplified in such OGCBMs to avoid high computational costs. In a similar fashion to inorganic carbon speciation, we outline a means by which the complex speciation of Fe can be included in global OGCBMs in a reasonably cost-effective manner. We use our Fe speciation to suggest the global distribution of different Fe species is tightly controlled by environmental variability (temperature, light, oxygen and pH) and the assumptions regarding Fe binding ligands. Impacts on bioavailable Fe are highly sensitive to assumptions regarding which Fe species are bioavailable. When forced by representations of future ocean circulation and climate we find large changes to the speciation of Fe governed by pH mediated changes to redox kinetics. We speculate that these changes may exert selective pressure on phytoplankton Fe uptake strategies in the future ocean. We hope our modeling approach can also be used as a “test bed” for exploring our understanding of Fe speciation at the global scale.

1 Introduction

The role of the micronutrient iron (Fe) in governing phytoplankton growth and primary production in large parts of the ocean is now well established (e.g., Boyd et al., 2007). One Fe-limited region of particular interest is the Southern Ocean, which plays an important role in governing air-sea CO₂ fluxes (Takahashi et al., 2009) and is predicted to be impacted heavily by climate change (e.g., Sarmiento et al., 2004). Accordingly, most current generation three-dimensional global Ocean General Circulation and Biogeochemistry Models (OGCBMs) that seek to explore the controls upon the cycling of

BGD

8, 2775–2810, 2011

Towards accounting for dissolved iron speciation

A. Tagliabue and
C. Völker

Title Page

Abstract

Introduction

Conclusions

References

Tables

Figures

⏪

⏩

◀

▶

Back

Close

Full Screen / Esc

Printer-friendly Version

Interactive Discussion

carbon and other nutrients, or the response of the ocean system to climate change typically all include Fe as a limiting nutrient for phytoplankton (e.g., Aumont and Bopp, 2006; Moore and Braucher, 2008; Galbraith et al., 2010). However, the cycle of Fe in seawater is highly complex, with nominally “dissolved” Fe (dFe) able to exist as many different species, not all bioavailable to phytoplankton (e.g., Hutchins et al., 1999; Maldonado et al., 2006).

dFe can be present as free inorganic Fe(II) and Fe(III), with redox transformations controlled by Fe(II) oxidation and Fe(III) reduction, themselves dictated by oxygen concentrations, superoxide concentrations, temperature, and pH (e.g., Santana-Casiano et al., 2005). Dissolved Fe(III) itself is highly insoluble in seawater and is generally found as colloidal Fe(III), or as soluble Fe(III) complexed to one or more organic ligands. Using electrochemical techniques it has been shown that over large parts of the world ocean > 99% of dFe is actually complexed to organic ligands of typically unknown provenance (e.g., Gledhill and van den Berg, 1994; Van den Berg, 1995; Rue and Bruland, 1995; Boye et al., 2003, 2006). This is important as it prevents the precipitation/scavenging of free inorganic Fe(III) to solid forms, which are effectively lost from the dissolved pool and bioavailable Fe species. Fe ligands thus increase both the solubility and residence time of dFe in the ocean, as well as exerting a control on its bioavailability. It appears likely that phytoplankton can access organically bound Fe, but this is by no means ubiquitous and the precise mechanisms involved remain debatable (e.g., Hutchins et al., 1999; Shaked et al., 2005; Maldonado et al., 2006; Salmon et al. 2006; Morel et al., 2008). Organically bound, as well as inorganic colloidal, Fe(III) can also be photoreduced in the presence of light to produce Fe(II) (e.g., Barbeau et al., 2003; Croot et al., 2008). As such, the speciation, residence time and bioavailability of Fe in the ocean depend on a suite of processes that are themselves highly sensitive to the environmental conditions of the ocean.

In the context of its complex speciation and cycling, dFe is treated very simply in “state-of-the-art” OGCBMs, with only a single dFe pool represented and ligand complexation accounted for assuming a single ligand of uniform concentration (e.g., Parekh

BGD

8, 2775–2810, 2011

Towards accounting for dissolved iron speciation

A. Tagliabue and
C. Völker

Title Page

Abstract

Introduction

Conclusions

References

Tables

Figures

⏪

⏩

◀

▶

Back

Close

Full Screen / Esc

Printer-friendly Version

Interactive Discussion

et al., 2004; Aumont and Bopp, 2006; Moore and Braucher, 2008; Galbraith et al., 2010). Spatio-temporal variability in Fe speciation, cycling and bioavailability is therefore ignored. Alongside the lack of constraints from observations, this is mostly due to the prohibitive computational cost of simulating rapid Fe cycle reactions at the global scale. Three-dimensional regional models have modeled the Fe cycle in a prognostic fashion for Fe-limited waters and noted the potential role of environmental variability in governing the supply of Fe to phytoplankton (Tagliabue and Arrigo, 2006). Similar models have also been employed in a one-dimensional framework at time series sites in the subtropical and tropical Atlantic Ocean (Weber et al., 2005, 2007; Ye et al., 2009). Recently, Tagliabue et al. (2009) included the first order impact of light and temperature on Fe speciation in a 3-D OGCBM and suggested that the role of environmental variability in Fe speciation could be important in governing the residence time and bioavailability of dFe in the ocean.

Over the coming century, the ocean is predicted to undergo a great deal of environmental change, especially the Fe-limited Southern Ocean. It is likely that temperatures will rise, stratification will increase, light levels will increase, pH will fall (due to the uptake of anthropogenic CO₂) and reduced sea ice will extend the growing season. All of these changes might impact upon the speciation of Fe and some experimental evidence from mesocosm experiments indeed suggests “acidification” induces changes to Fe(II) levels (Breitbarth et al., 2010), while laboratory experiments using synthetic ligands lead to modifications to Fe bioavailability that depend upon the type of chelator considered (Shi et al., 2010). As it stands, even including the first order impact of light and temperature on the marine Fe cycle (as per Tagliabue et al., 2009) will not resolve the matrix of parallel changes resulting from climate change that will impact Fe cycle rate processes (e.g., oxidation rates, photoreduction rates), the dFe concentration itself and the concentration of ligands. To address these questions we require a tool that can resolve the speciation of Fe in a semi-prognostic manner at the global scale in a “cost effective” manner. In this study, we outline a new approach that permits the “semi-prognostic” modeling of Fe speciation at the global scale using an analytical

Towards accounting for dissolved iron speciation

A. Tagliabue and
C. Völker

Title Page

Abstract

Introduction

Conclusions

References

Tables

Figures



Back

Close

Full Screen / Esc

Printer-friendly Version

Interactive Discussion



approach similar to that typically employed for inorganic carbon speciation. We then use this model to speculate how Fe speciation might respond to the climate associated with an atmospheric CO₂ concentration of ~ 1000 ppm as an illustration of how our Fe speciation model can be applied.

2 Theoretical framework

Our approach rests on the concept of “fast” and “slow” Fe cycle reactions that assumes, similar to modules that compute inorganic carbon speciation in OGCBMs, that there are a subset of “fast” Fe speciation reactions that approach equilibrium within the time step of the model (normally around one to two hours). For example, the chemical reactions that govern dFe speciation (oxidation, photoreduction, the formation and dissociation of Fe-ligand complexes etc.) are assumed to be “fast” reactions. Examples of “slow” reactions that would need to be computed prognostically by the OGCBM include scavenging of free inorganic Fe(III) onto particles or uptake and recycling of Fe by biology. We assume dFe speciation to be a “fast” problem and therefore well suited to similar analytical approaches as have been successfully employed in OGCBMs that seek to compute inorganic carbon speciation for air-sea CO₂ exchange or pH calculations.

The full equations of the dFe model used here are presented in Tagliabue and Arrigo (2006) and Tagliabue et al. (2009). The state variables of the model are the free concentrations of Fe(II) (Fe(II)'), Fe(III) (Fe(III)'), Fe(III) bound to the weak non-bioavailable ligand (FeL_W) and the strong bioavailable ligand (FeL_S), solid Fe(III) (Fe_p), the total dFe concentration (Fe_T), the uncomplexed weak (L_W) and strong (L_S) ligands and the total concentration of L_W (L_{WT}) and L_S (L_{ST}). We disregard here complexation of Fe(II) by organic ligands. Ferrous iron complexes have been suggested to be possibly responsible for the long residence time of Fe(II) in the SOIREE iron fertilization experiment (Croot et al., 2001), but have only been demonstrated in riverine or coastal waters with high fulvic acid concentrations (Voelker and Sulzberger, 1996; Rose and Waite, 2003). However, such Fe(II) specific ligands may be difficult to identify using current

Towards accounting for dissolved iron speciation

A. Tagliabue and
C. Völker

Title Page

Abstract

Introduction

Conclusions

References

Tables

Figures



Back

Close

Full Screen / Esc

Printer-friendly Version

Interactive Discussion



techniques when they are at low abundance (e.g., Croot et al., 2007, 2008). Rate constants required by the model are the oxidation of $\text{Fe(II)'} (k_{\text{ox}}$, which is a function of temperature, pH, salinity and oxygen concentrations), photoreduction of $\text{FeL}_W (k_{\text{phW}}$, which is a function of irradiance as per Tagliabue et al., 2009) and $\text{FeL}_S (k_{\text{phS}}$, the formation of $\text{FeL}_W (k_{\text{IW}}$) and $\text{FeL}_S (k_{\text{IS}}$), the dissociation of $\text{FeL}_W (k_{\text{bW}}$) and $\text{FeL}_S (k_{\text{bS}}$), the precipitation of $\text{Fe(III)'} (k_{\text{pcp}}$) and the remineralization of $\text{Fe}_P (k_r)$. Re-arranging the differential equations for the Fe species results in the following four governing equations:

$$0 = k_{\text{IW}}\text{Fe(III)'}_W - k_{\text{bW}}\text{FeL}_W - k_{\text{phW}}\text{FeL}_W \quad (1)$$

$$0 = k_{\text{IS}}\text{Fe(III)'}_S - k_{\text{bS}}\text{FeL}_S - k_{\text{phS}}\text{FeL}_S \quad (2)$$

$$0 = k_{\text{phW}}\text{FeL}_W + k_{\text{phS}}\text{FeL}_S - k_{\text{ox}}\text{Fe(II)'} \quad (3)$$

$$0 = k_{\text{pcp}}\text{Fe(III)'} - k_r\text{Fe}_P \quad (4)$$

Additional constraints are that the concentrations of Fe_T , L_{WT} and L_{ST} must be conserved over the fast timescale:

$$\text{Fe}_T = \text{Fe(III)'} + \text{Fe(II)'} + \text{FeL}_W + \text{FeL}_S + \text{Fe}_P \quad (5)$$

$$L_{WT} = \text{FeL}_W + L_W \quad (6)$$

$$L_{ST} = \text{FeL}_S + L_S \quad (7)$$

In order to solve the model analytically first requires a rearrangement of Eqs. (3) and (4) to yield:

$$\text{Fe(II)'} = \frac{k_{\text{phW}}}{k_{\text{ox}}}\text{FeL}_W + \frac{k_{\text{phS}}}{k_{\text{ox}}}\text{FeL}_S \quad (8)$$

and

$$\text{Fe}_P = \frac{k_{\text{pcp}}}{k_r}\text{Fe(III)'} \quad (9)$$

Towards accounting for dissolved iron speciation

A. Tagliabue and
C. Völker

Title Page

Abstract

Introduction

Conclusions

References

Tables

Figures

◀

▶

◀

▶

Back

Close

Full Screen / Esc

Printer-friendly Version

Interactive Discussion

These equations are then inserted into Eq. (5) to result in:

$$\text{Fe}_T = a\text{Fe(III)}' + b\text{FeL}_W + c\text{FeL}_S \quad (10)$$

where $a = 1 + k_{\text{pcp}}/k_r$, $b = 1 + k_{\text{phW}}/k_{\text{ox}}$, and $c = 1 + k_{\text{phS}}/k_{\text{ox}}$. From Eqs. (6) and (7) it follows that the free ligand concentrations are:

$$L_W = L_{WT} - \text{FeL}_W \quad (11)$$

$$L_S = L_{ST} - \text{FeL}_S. \quad (12)$$

Equation (12) can now be used in combination with Eq. (2) to produce:

$$0 = k_{\text{IS}}\text{Fe(III)}'(L_{ST} - \text{FeL}_S) - (k_{\text{bS}} + k_{\text{phS}})\text{FeL}_S \quad (13)$$

and solved for FeL_S :

$$\text{FeL}_S = \frac{\text{Fe(III)}'L_{ST}}{K_S + \text{Fe(III)}'} \quad (14)$$

where $K_S = (k_{\text{bS}} + k_{\text{phS}})/k_{\text{IS}}$. Equation (14) is then combined with Eq. (10) to solve for the concentration of FeL_W :

$$\begin{aligned} \text{FeL}_W = k_{\text{IW}}\text{Fe(III)}' \left(L_{WT} - \frac{\text{Fe}_T}{b} + \frac{a\text{Fe(III)}'}{b} + \frac{c\text{Fe(III)}'}{b} \frac{L_{ST}}{K_S + \text{Fe(III)}'} \right) \\ - (k_{\text{bW}} + k_{\text{phW}}) \left(\frac{\text{Fe}_T}{b} - \frac{a\text{Fe(III)}'}{b} - \frac{c\text{Fe(III)}'}{b} \frac{L_{ST}}{K_S + \text{Fe(III)}'} \right) \end{aligned} \quad (15)$$

Inserting Eq. (15) into Eq. (1) permits us to obtain an equation for $\text{Fe(III)}'$ which, after simplification and sorting into powers of $\text{Fe(III)}'$, yields a third order polynomial solution for the concentration of $\text{Fe(III)}'$:

$$0 = (\text{Fe(III)}')^3 + \left(\frac{bL_{WT}}{a} + \frac{cL_{ST}}{a} + K_S + K_S - \frac{\text{Fe}_T}{a} \right) (\text{Fe(III)}')^2$$

**Towards accounting
for dissolved iron
speciation**

A. Tagliabue and
C. Völker

Title Page

Abstract

Introduction

Conclusions

References

Tables

Figures

⏪

⏩

◀

▶

Back

Close

Full Screen / Esc

Printer-friendly Version

Interactive Discussion



$$\begin{aligned}
 & + \left(K_S \frac{bL_{WT}}{a} + K_W \frac{cL_{ST}}{a} + K_W K_S - (K_W + K_S) \frac{Fe_T}{a} \right) Fe(III)' \\
 & - K_W K_S \frac{Fe_T}{a}
 \end{aligned}
 \tag{16}$$

where $K_W = (k_{bW} + k_{pHw})/k_{1W}$. Equation (16) can be solved analytically or iteratively and has three solutions, but only one is positive and thus a realizable $Fe(III)'$ concentration. Therefore by first solving Eq. (16) for the $Fe(III)'$ concentration, one can then proceed to solve for the Fe_P concentration (Eq. 9), FeL_S concentration (Eq. 14), FeL_W concentration (Eq. 15), and finally the $Fe(II)'$ concentration (Eq. 8). Thus for a given set of rate constants, which are either fixed or vary as a function of environmental variables, and the concentrations of Fe_T , L_{WT} , L_{ST} , the procedure outlined above analytically solves for the concentrations of the 5 Fe species ($Fe(II)'$, $Fe(III)'$, FeL_W , FeL_S , and Fe_P) at considerably less computational expense than a prognostic solution. In “offline” tests only using the chemistry module, we find that the analytical solution provides an identical speciation solution as that from a fully prognostic version of the same model.

3 Inclusion in an OGCBM

3.1 Modeling framework and experiments

We decided to include our analytical solution for dFe speciation within the PISCES OGCBM (Aumont and Bopp, 2006), since this model has been widely used for ocean biogeochemistry and climate applications, including some addressing Fe speciation (e.g., Tagliabue et al., 2009). Firstly, the analytical solution of equation 16 was solved iteratively in each grid cell of the model at each time step to yield the $Fe(III)'$ concentration. From this, the concentrations of all other Fe species can then be computed. The analytical solution uses properties that are either provided by the PISCES model (Fe_T ,

BGD

8, 2775–2810, 2011

Towards accounting for dissolved iron speciation

A. Tagliabue and
C. Völker

Title Page

Abstract

Introduction

Conclusions

References

Tables

Figures

⏪

⏩

◀

▶

Back

Close

Full Screen / Esc

Printer-friendly Version

Interactive Discussion



Towards accounting for dissolved iron speciation

A. Tagliabue and
C. Völker

Title Page

Abstract

Introduction

Conclusions

References

Tables

Figures

◀

▶

◀

▶

Back

Close

Full Screen / Esc

Printer-friendly Version

Interactive Discussion



L_{WT} , L_{ST}) or computed in each grid cell and at each time step from variables simulated by the PISCES model (k_{ox} , k_{pHw} , k_{pHS} , k_{IW} , k_{IS} , k_{bW} , k_{bS} , k_{pcp} and k_r). For example, k_{ox} will vary in space and time as a function of the temperature, pH, oxygen concentration, and salinity, following the equation of Santana-Casiano et al. (2005), while k_{pHw} and k_{pHS} will vary with depth and season following available radiation at each particular model grid cell (all other rate constants are initially fixed in space and time). The total dFe pool is also modified each time step by phytoplankton uptake and remineralisation and all other source – sink terms for dFe traditionally included in the PISCES model (see: Aumont and Bopp, 2006 for a full list of Fe equations). We find that the calculated Fe_T computed from the sum of all species calculated analytically is generally less than $\pm 1\%$ in error relative to the dFe tracer prognostically simulated by PISCES (which is an input to the speciation solution) and only reaches a maximum of $\pm 5\%$ error in a few isolated grid cells (below 75 m and 150 m the error is less than $\pm 1\%$ and $\pm 0.1\%$, respectively). This demonstrates that our procedure has an acceptable error in calculating Fe speciation, especially considering the global nature of its application and the necessity to retain a degree of computational efficiency.

3.2 Rate constants

Values for the rate constants are taken from the published literature and, apart from the examples detailed here, are identical to those described by Tagliabue et al. (2009). For this study, we used the k'_{ox} equation (s^{-1}) as described by Santana-Casiano et al. (2005), which is a function of temperature, salinity and pH:

$$\log_{10} k'_{ox} = 35.407 - 6.7109 \text{ pH} + 0.5342 \text{ pH}^2 - 5362.6 \text{ Tk} - 0.04406 S^{0.5} - 0.002847 S \quad (17)$$

Where Tk is the temperature in K, pH is the pH (free scale) and S is salinity. The realised rate of Fe(II) oxidation (k_{ox}) is then modified by the oxygen (mol L^{-1}) concentration (J. Santana-Casiano and M. Gonzalez-Davila, personal communication, 2010) using

$$k_{ox} = k'_{ox} / O_{2 \text{ sat}} \cdot O_2 \quad (18)$$

The kinetic characteristics of L_W are assumed to be similar to Phaeophytin-type ligands and rate constants are taken from Witter et al. (2000), with a log conditional stability ($\log(k_{1W}/k_{bW})$) of 11.00 M^{-1} . L_S is assumed to have the kinetic characteristics of desferrioxamine B-type ligands (Witter et al., 2000) with a log conditional stability of 12.12 M^{-1} . In the absence of other information, the kinetic characteristics of L_W and L_S are fixed in space and time, and are within the range of measurements made in situ for “strong” and “weak” ligands (e.g., Rue and Bruland, 1995; Boye et al., 2003; 2006; Cullen et al., 2006). Initially we define “bioavailable” dFe (bFe) as the sum of $\text{Fe(II)}'$, $\text{Fe(III)}'$ and FeL_S .

3.3 Parameterisation of Fe binding ligands

Most OGCBMs assume that the concentration of dFe binding ligands is fixed at between 0.6 and 1 nM and only assume one fully bioavailable ligand is present (e.g., Aumont and Bopp, 2006; Moore and Braucher, 2009; Tagliabue et al., 2009; Galbraith et al., 2010). Nevertheless, there is ample experimental evidence of at least two ligand classes and highly variable concentrations (e.g., Buck and Bruland, 2007; Hunter and Boyd, 2007). While parameterizing the sources and sinks of two ligand classes in an OGCBM is perhaps out of reach at this moment (it has been done for a one-dimensional model, Ye et al., 2009), there is some data showing an relationship between ligands and dissolved organic carbon (DOC) concentrations (Wagener et al., 2008, see also: Hiemstra and van Riemsdijk, 2006). We therefore decided to use the relationship from the observations of Wagener et al. (2008) to permit us to have ligand concentrations that vary as a function of total DOC concentrations (DOC_{TOT} , in $\mu\text{mol L}^{-1}$) that are already prognostically simulated by PISCES.

$$L_T = L_{WT} + L_{ST} = (\text{DOC}_{\text{TOT}} \cdot 0.09) - 3.2 \quad (19)$$

PISCES includes a semi-labile DOC pool as a prognostic tracer (Aumont et al., 2001) and we therefore assume a constant refractory DOC pool of $40 \mu\text{M}$ to arrive at a total DOC concentration (DOC_{TOT}). Sources of DOC (and thus sources of ligands) in our

BGD

8, 2775–2810, 2011

Towards accounting for dissolved iron speciation

A. Tagliabue and
C. Völker

Title Page

Abstract

Introduction

Conclusions

References

Tables

Figures

⏪

⏩

◀

▶

Back

Close

Full Screen / Esc

Printer-friendly Version

Interactive Discussion



Towards accounting for dissolved iron speciation

A. Tagliabue and
C. Völker

[Title Page](#)[Abstract](#)[Introduction](#)[Conclusions](#)[References](#)[Tables](#)[Figures](#)[⏪](#)[⏩](#)[◀](#)[▶](#)[Back](#)[Close](#)[Full Screen / Esc](#)[Printer-friendly Version](#)[Interactive Discussion](#)

model are exudation during photosynthesis, zooplankton grazing, disaggregation of particles etc., with DOC lost due to bacterial activity and aggregation. Observations show ligand concentration minima of 0.4 nM at 40 μ M DOC (Wagener et al., 2008). So following the philosophy of Hunter and Boyd (2007), we set the minimum L_W concentration to be 0.4 nM at 40 μ M DOC (representing a “refractory” weak ligand pool), and for DOC concentrations greater than 40 μ M we portioned two thirds of the “extra” ligand into L_S and one third into L_W . In this fashion we account for the active production of strong ligands (L_S) by the euphotic zone biotic community, as well as subsurface production of weak ligands (L_W) in a relatively simple fashion. The spatial distribution of L_T using our DOC-linked parameterization is shown in Fig. 1, in subsurface waters values are around 0.4–0.6 nM.

3.4 Model experiments

We decided to use our Fe speciation OGCBM to conduct some illustrative model experiments. We firstly simulated Fe chemistry for the “present” climate using an atmospheric CO_2 level of 368.87 ppm (corresponding to observations from the year 2000), an ocean circulation from NEMO that arises from atmospheric re-analysis products (Aumont et al., 2008) and depart from a simulation conducted from 1860–2000 forced by atmospheric CO_2 observations (to ensure a correct ocean pH). Initially, we used the parameterisation of the Fe cycle as described as above, but we also conducted some illustrative sensitivity tests to examine assumptions regarding the nature of the variability associated with the Fe binding ligand pool. Finally, in order to appraise the possible impact of climate change on Fe speciation, we used 2 representations of ocean circulation, as well as initialization files for ocean biogeochemistry (to include the requisite DIC and pH changes), from the IPSL-CM5 coupled model at atmospheric CO_2 levels of 298.06 ppm and 1086.64 pmm (from a transient coupled simulation from pre-industrial CO_2 levels to $4 \times \text{CO}_2$) and conducted 10 yr simulations with the Fe speciation analytical solution included in PISCES.

4 Results of the model

4.1 Fe speciation from the standard model and comparison with observations

General Fe speciation. Figure 2 illustrates the Fe speciation that results from the standard parameterization of our Fe model under modern climatic forcing. Annually averaged Fe(II) distributions generally track those of dFe (Fig. 2a,b) and over most of the ocean range between 0 and 100 pM. The annual mean (seasonal variability in pFe(II) is discussed below) proportion of the dFe pool present as Fe(II) (pFe(II)) ranges from 0 to around 30% and is maximal at high latitudes (10–30%), moderate in upwelling regions (3–4%) and very low in the tropical oceans (< 1%) (Fig. 2c). For example, pFe(II) increases as one moves south in the Southern Ocean from < 5% near South Africa to ~ 30% at around 55° S, with similar degree of change in the high latitude Northern Oceans (Fig. 2c). In general, the latitude-longitude variability in pFe(II) is tightly linked to the variability in k_{ox} for the surface ocean (Fig. 2d). Irradiance governs the depth distribution of pFe(II), with Fe(II) only making up an appreciable fraction of dFe at depths shallower than ~ 100 m (Fig. 3a). An exception to this are suboxic zones, wherein the reduction in k_{ox} results in Fe(II) levels > 100 pM (Fig. 3b, 200–300 m). Organically complexed Fe(III) (Fe_{L_S} and Fe_{L_W}) makes up almost 100% of the dFe pool over most of the global ocean, declining slightly to around 85% in polar waters where Fe(II) is greater due to supply from photoreduction and reduced oxidation rates.

Bioavailable Fe. bFe shows variability that is linked to photochemistry, organic complexation and irradiance, as well as being highly sensitive to which species are assumed to be bioavailable. If bFe is assumed to encompass Fe(II), Fe(III) and $Fe(III)_{L_S}$ then the proportion of the dFe pool present as bFe (pbFe) varies between 50 to 90% in surface waters (when annually averaged, Fig. 4a). Variability in pbFe at the surface is positively related to irradiance (due to greater photoproduction of Fe') and the total ligand concentration (due to reduced losses as Fe_P) and is negatively related to the dFe concentration (due to over-saturation of ligands and loss as Fe_P) (Fig. 4b–d). pbFe declines with depth due to the reduced irradiance and lower ligand concentrations at

BGD

8, 2775–2810, 2011

Towards accounting for dissolved iron speciation

A. Tagliabue and
C. Völker

Title Page

Abstract

Introduction

Conclusions

References

Tables

Figures

⏪

⏩

◀

▶

Back

Close

Full Screen / Esc

Printer-friendly Version

Interactive Discussion



depth (at least in our DOC-based ligand parameterization). If we assume that only Fe(II) and Fe(III) are assumed to make up bFe, then the reduction in pbFe is striking (Fig. 5). Only at high latitudes, where Fe(II) is greatest (Fig. 2a), can pbFe approach even 25% of the dFe pool and over large parts of the ocean pbFe is < 5% of dFe (Fig. 5). This is due to the reduced residence time for Fe' (the sum of Fe(II) and Fe(III)) away from polar waters and would imply that phytoplankton reliant on Fe' would be chronically Fe limited in these waters (Tagliabue et al., 2009). Accordingly, pbFe is strongly and negatively related to spatial variability in Fe(II) oxidation rates when $bFe = Fe(II) + Fe(III)$, and thus generally tracks variability in pFe(II).

Importance of seasonality. Seasonality plays an important role in Fe speciation, especially at high latitudes where there are large changes in environmental variables (temperature, irradiance etc., Tagliabue and Arrigo, 2006). During the winter-spring transition in the high latitude Northern and Southern Hemispheres we suggest an increase in pFe(II) that is maximal in October-December in the Southern Ocean and June-July in the North Atlantic and sub-Arctic Pacific (Fig. 6a). Similarly, pbFe also increases from winter to spring as mixed layers shallow and irradiance levels are increased (Fig. 6b). For the Fe-limited Southern Ocean, pbFe increases from ~ 50% in winter (due to sea-ice or very deep winter mixed layers) to ~ 80% by spring when waters are ice-free and characterized by well-lit stratified surface waters. Parallel to the increasing Fe(II), the organically complexed fraction of dFe declines between winter and spring.

Comparison with observations. The most obvious and widespread dataset with which to compare the model is the simulated dFe concentration (from the sum of the Fe species computed by our speciation model). This compares well to a new database of ~ 13 000 dFe measurements (Tagliabue, 2011, $R = 0.52$ and 0.54 for the entire water column and 0–50 m, respectively), but although this shows our speciation model does not give unrealistic dFe concentrations in general, the good statistical reproduction of dFe probably more reflects the successful simulation of dFe in PISCES. Fe speciation measurements are obviously rarer than those for dFe, but one candidate to compare

BGD

8, 2775–2810, 2011

Towards accounting for dissolved iron speciation

A. Tagliabue and
C. Völker

Title Page

Abstract

Introduction

Conclusions

References

Tables

Figures

◀

▶

◀

▶

Back

Close

Full Screen / Esc

Printer-friendly Version

Interactive Discussion

**Towards accounting
for dissolved iron
speciation**A. Tagliabue and
C. Völker

[Title Page](#)[Abstract](#)[Introduction](#)[Conclusions](#)[References](#)[Tables](#)[Figures](#)[⏪](#)[⏩](#)[◀](#)[▶](#)[Back](#)[Close](#)[Full Screen / Esc](#)[Printer-friendly Version](#)[Interactive Discussion](#)

our speciation model to is Fe(II). At high latitudes, the model appears to do a good job, with surface Fe(II) concentrations of ~ 25 pM south of New Zealand comparing well with a range of 19–46 pM from Croot et al. (2007) and modeled values of ~ 30 –60 pM from the western sub-Arctic Pacific within the range of ~ 20 –40 pM from Roy et al. (2008), with Fe(II) observations making up as much as 50% of the dFe pool (modeled values are 30–40%). In addition, the depth profile from Roy et al. (2008) is also relatively well reproduced by the model, except for the reduced attenuation of Fe(II) with depth in the model (Fig. 7). Earlier Southern Ocean observations of 0–45 pM using a towed fish (Bowie et al., 2002) are also reasonably well reproduced by the model. A widespread Fe(II) dataset was obtained by Sarthou et al. (2011) along the Bonus-GoodHope transect in the Southern Ocean and using the parallel dFe measurements (Chever et al., 2010) permits us to derive pFe(II). Our model does a good job in reproducing the general values of surface Fe(II) observed in the Southern Ocean (0–40 pM vs. 12–116 pM), as well as the increasing southward trend along the Bonus-GoodHope line (Sarthou et al., 2011). In addition, pFe(II) from the model (0–30% increasing southward) agrees well with the observations (3–67%, Sarthou et al., 2011). It is noteworthy, that the observed latitudinal trends in both Fe(II) and pFe(II) were only significant for daytime stations (Fe(II)) and for both daytime and all stations (pFe(II)), but never when only night-time stations were considered (Sarthou et al., 2011). In the eastern North Atlantic, the onshore-offshore trend (from >250 to 100–150 pM) observed by Boye et al. (2003) is well reproduced by the model and observed offshore values (~ 100 pM) are, in general, only slightly underestimated by the model (although the limit of detection in Boye et al. (2003) was 100 pM). This is probably due to the onshore-offshore trend in dFe concentrations, since we do not include a specific source of Fe(II) at the margin (there is a margin source of dFe in PISCES). High modeled Fe(II) levels in the Baltic Sea agree well with measurements of Breitbarth et al. (2009). In general, this suggests that the model is reproducing the dominant processes governing the Fe(II) distribution in higher latitude Atlantic, Pacific and Southern Oceans.

The model does a poorer job when compared to the comprehensive lower latitude Pacific Ocean measurements of Hansard et al. (2009) along $\sim 30^\circ$ N (line P02) and $\sim 152^\circ$ W (line P16N), with observed values of > 30 pM (as high as > 100 pM in some places) greatly underestimated by the model (generally < 5 pM). This could be due to either differences in methods to other studies, errors in the modeled dFe field (which is closely linked to absolute Fe(II) concentrations, Fig. 2b), processes missing in our speciation model, a lack of high frequency output, or the absence of the diurnal cycle in PISCES. The method employed by Hansard et al. (2009) is based on acidified samples and therefore likely reflects a labile Fe' pool that is highly sensitive to redox conditions. Unfortunately, the dFe measurements taken parallel to the Hansard et al. (2009) Fe(II) measurements are not yet available and it is not possible to directly compare pFe(II) from the model and observations (which would tell us if the error was mostly "speciation" based). Nevertheless, pFe(II) values of 5–25% reported by Hansard et al. (2009) are underestimated by our model. dFe concentrations from the model along the P02 and P16N transects are between 50 and 100 pM and are therefore very low, relative to the Fe(II) concentrations measured by Hansard et al. (2009), which are of the same order. This suggests it would be very difficult to achieve any appreciable Fe(II) in this region whilst modeled dFe values remain so low. Additional sensitivity tests focused on producing more Fe(II) in this region (drastically reducing k_{ox} or increasing photoreduction, not shown) do not permit any appreciable accumulation of Fe(II) therein and result in unrealistically high Fe(II) concentrations in the high latitudes. Fe(II) might also be underestimated in the lower latitude ocean because the diurnal cycle in irradiance is not included in our OGCBM. Another important issue to bear in mind is that we compare point measurements to the monthly mean model output. Models and observations (e.g., Bowie et al., 2002; Tagliabue and Arrigo, 2006; Croot et al., 2007, 2008; Roy et al., 2008; Breitbath et al., 2009; Ye et al., 2009; Sarthou et al., 2011) show a high degree of variability in Fe(II) in response to changing environmental conditions (especially solar radiation on the diel cycle), although it is noticeable that Hansard et al. (2009) note no diurnal cycle in their observations, in contrast to other studies.

Towards accounting for dissolved iron speciation

A. Tagliabue and
C. Völker

Title Page

Abstract

Introduction

Conclusions

References

Tables

Figures

⏪

⏩

◀

▶

Back

Close

Full Screen / Esc

Printer-friendly Version

Interactive Discussion



Our model may not capture these “extreme” events that are highly specific to the time and location of each precise sample. This is because despite a 1.5 h timestep, we do not include the diurnal cycle and compare monthly mean modeled Fe(II) to point measurements. Therefore, we must conclude that a combination of a very low modeled dFe concentration, lack of high frequency variability and perhaps also an impact of acidified samples and errors in our formulated Fe cycle (see below) precludes a good reproduction of the reported Fe(II) data in the subtropical Pacific Ocean (Fe(II) levels are higher in the tropical Atlantic due to greater dust input of dFe). However we do note the increased Fe(II) in suboxic zones (Fig. 3b), in the eastern tropical Pacific in particular, that compare well to measured increases in Fe(II) at low oxygen levels (e.g., Hopkinson and Barbeau, 2007).

As regards the degree of organic complexation, our results of virtually 100% complexation of dFe agrees with all available observations (e.g., Boye et al., 2003, 2006; Buck and Bruland, 2007) and lesser complexation where Fe inputs are high is in accord with the findings from an artificial Fe enrichment experiment (Boye et al., 2005). Overall, our speciation model can be seen to do a much better job at higher latitudes, rather than lower latitudes without significant Fe inputs (where Fe(II) levels appear too low).

Sensitivity tests. If we assume that Fe binding ligands are fixed in space and time, then we find that Fe speciation and cycling is modified. For example, fixing ligands at 0.6 nM results in a lower ligand concentration over much of the ocean than from our DOC-based parameterization (Fig. 1). A lower ligand concentration unsurprisingly results in a reduction in the proportion of the total dFe pool that is organically complexed (Fig. 8a). This then impacts the total dFe pool, which is reduced (due to greater losses as Fe_P), especially in regions of high Fe inputs (beneath zones of dust deposition and near coasts). The impact of fixed (and generally lower) ligand concentrations upon bFe depends on the assumed make up of the bFe pool. If $bFe = Fe(II) + Fe(III) + FeL_S$, then bFe declines if ligands are fixed (Fig. 8b), due to reduced stabilization of bFe by L_S (as its concentration is reduced). On the other hand, if bFe is assumed to be only made

BGD

8, 2775–2810, 2011

**Towards accounting
for dissolved iron
speciation**A. Tagliabue and
C. Völker

Title Page

Abstract

Introduction

Conclusions

References

Tables

Figures

⏪

⏩

◀

▶

Back

Close

Full Screen / Esc

Printer-friendly Version

Interactive Discussion

up of Fe(II) and Fe(III), then assuming lower and fixed ligand concentrations actually increases bFe (albeit from very low levels, Fig. 8c), particularly in areas of high Fe input, due to lesser complexation by organic ligands (which are assumed inaccessible to phytoplankton in this formulation of bFe). Thus the nature of the ocean ligand pool has impacts upon the general speciation of Fe, as well as its residence time and bioavailability. We reiterate that for phytoplankton that can access organically complexed Fe, bFe declines when ligands are fixed (at generally lower levels than measured), while for phytoplankton reliant on inorganic Fe, bFe increases when ligands are fixed since more Fe is in inorganic forms.

4.2 Fe speciation at four times CO₂

At atmospheric CO₂ levels of approximately 1000 ppm the environmental properties of the ocean are unsurprisingly greatly modified. In general, and similar to previous studies with fully coupled climate-OGCBMs (e.g., Steinacher et al., 2010), the surface ocean is warmer, more stratified (reduced mixed layer depth) and has a lower pH. In the Southern Ocean, sea ice coverage is also reduced which lengthens the growing season. Our objective here is not to comprehensively analyze these aspects (this is for other more focused papers), but to examine how Fe speciation changes using our analytical approach.

Turning firstly to Fe(II), we find large increases in pFe(II) (chosen to remove the effect of climate on absolute dFe concentrations) due to climate change that are maximal in the high latitude oceans (Fig. 9a). pFe(II) increases by as much as > 40% in the high latitude Southern and Northern Oceans (Fig. 9a) and must be responding to changes to oxidation and photoreduction rates. However, a closer inspection reveals that the largest changes in pFe(II) occur where photoreduction rates were not significantly changed and that there is a very close relationship between the predicted changes to pFe(II) and oxidation rates (Fig. 9b). This suggests that the impact of reduced pH is overriding the impact of greater temperature to yield a net reduction in the future oxidation rate of Fe(II), especially in the high latitude oceans. Similar accumulations of

Towards accounting for dissolved iron speciation

A. Tagliabue and
C. Völker

Title Page

Abstract

Introduction

Conclusions

References

Tables

Figures



Back

Close

Full Screen / Esc

Printer-friendly Version

Interactive Discussion



Fe(II) at lower pH were obtained in mesocosm experiments by Breitbarth et al. (2010), where pH changes impacting oxidation rates were also found to be the dominant effect.

Modifications to the Fe(II) concentrations due to high CO₂ induced changes to oxidation rates have implications for the speciation and bioavailability of Fe. Firstly, the greater proportion of the dFe pool present as Fe(II) reduces the amount of Fe that is complexed by organic ligands, but since this Fe is instead retained as Fe(II) species (rather than Fe(III)), there is not a great impact on losses of dFe as Fe_P. As for the modern climate, the impacts on pbFe depend upon the assumptions regarding the bFe pool. If $bFe = Fe(II) + Fe(III) + FeL_S$, then climate change and ocean acidification have only a modest impact on pbFe, with pbFe increasing by < 10% in the Fe-limited Southern Ocean or by up to 20% in the Arctic (Fig. 9c). This is because we assume all bFe (Fe(II), Fe(III), and FeL_S) species to be similarly bioavailable. On the other hand, if only Fe(II) and Fe(III) are assumed bioavailable, then large increases in pbFe, which parallel those in pFe(II), are found in the Fe-limited Southern Ocean (Fig. 9d) as more dFe now remains in the Fe(II) state, relative to organically complexed Fe(III) pool, due to the reduced oxidation rates. An implication of this result is that climate/acidification induced changes to Fe speciation (that primarily result from pH changes) might make phytoplankton that rely only on Fe(II) and Fe(III) more competitive in the future. It may be that the investment necessary to access organically complexed Fe (see e.g., Maldonado et al., 2006) would be thus less advantageous as a result of ocean acidification. For example, assuming a general half saturation constant (K_s) for growth as a function of Fe of 0.05 nM and defining waters as nominally “Fe limited” when the bFe concentration < K_s, we find that the “Fe limited” area of Southern Ocean surface waters (south of 40° S) either changes insignificantly (~ 0%) for phytoplankton that access organically complexed Fe or declines greatly (–17%) if only Fe(II) and Fe(III) are bioavailable. This illustrates the potential advantage that might accrue for phytoplankton species that eschew the cellular investment necessary to access organically complexed Fe in the future “acidified” ocean.

Towards accounting for dissolved iron speciation

A. Tagliabue and
C. Völker

[Title Page](#)[Abstract](#)[Introduction](#)[Conclusions](#)[References](#)[Tables](#)[Figures](#)[⏪](#)[⏩](#)[◀](#)[▶](#)[Back](#)[Close](#)[Full Screen / Esc](#)[Printer-friendly Version](#)[Interactive Discussion](#)

5 Future directions

5.1 Improvements to the speciation model

While our Fe speciation model is complex, relative to contemporary treatments of Fe cycling in global OGCBMs, there are a number of simplifications and processes that could be included/tested in the future. For example, processes such as Fe(III) reduction as mediated by superoxide, the direct photoreduction of Fe(III) and Fe(III) colloids, as well as including the role of superoxide and hydrogen peroxide in the oxidation of Fe(II) could also be important in governing the spatio-temporal variability in Fe(II) concentrations. The Fe speciation model of Ye et al. (2009) is a good candidate model with which to explore the potential importance of such processes. However, as this model is even more complex than our Fe speciation model, it cannot be solved analytically anymore. Nevertheless, an iterative numerical solution is possible and leads to vast savings in computational time compared to solving the full kinetic equations in the one-dimensional setting by Ye et al. (2009) (Voelker et al., 2011). A good candidate addition to the current speciation model that would not overcomplicate the analytical solution might be Fe(II) ligands, which could assist in reproducing the relatively high Fe(II) suggested in the low latitudes (e.g., Hansard et al., 2009). The presence of Fe(II) ligands has been noted in rainwater (e.g., Willey et al., 2008) and suggested in the open ocean as well (e.g., Croot et al., 2001) and their presence may assist in stabilising Fe(II) for a number of hours. It is not difficult to include an Fe(II)-binding ligand in the analytical solution presented here, but this would require more information on its specific binding strength, as well as its sources and concentration. Specific sources of Fe species could also be important, with observational studies also suggesting that continental margins and organic matter remineralisation can supply Fe(II) (Boye et al., 2006; Sarthou et al., 2011), likely stabilised to some degree. However, including and appraising Fe(II) sources is not possible in our analytical approach and would be better tested by fully prognostic, and thus necessarily regional, Fe speciation models. Nevertheless, our approach of separating the “fast” and “slow” Fe cycle reactions will permit

Towards accounting for dissolved iron speciation

A. Tagliabue and
C. Völker

Title Page

Abstract

Introduction

Conclusions

References

Tables

Figures



Back

Close

Full Screen / Esc

Printer-friendly Version

Interactive Discussion



us to test many question regarding the controls on Fe speciation in the global ocean during future studies such as the presence and cycling of Fe ligands, including perhaps those specific to Fe(II), and questions regarding Fe bioavailability (see below).

5.2 Modeling Fe binding ligands

5 We have shown that variability in ocean Fe binding ligands exert a critical control on the speciation of dFe and, as such, on the residence time and bioavailability of dFe. Here we have used the semi-labile DOC pool as simulated by PISCES, alongside a relationship derived from field observations (Wagener et al., 2008) to allow ligands to vary in our model. However, while this is likely to be a cost effective improvement upon
10 a fixed uniform ligand concentration (as currently employed in other OGCBMs), it will be important to carefully compare the distribution with widespread in situ ligand data (Boye et al., 2011) to better constrain its viability. For example, while our DOC-linked parameterization will account for ligand production in surface waters, remineralisation (Boyd et al., 2010) is not a source of ligands. In the future it may be useful to include
15 a prognostic simulation of the production of weak ligands from organic matter breakdown, as well as the production of strong ligands by the biota, possibly mediated by Fe stress as per Ye et al. (2009). A prognostic ligand model would need to be simulated as part of the “slow” Fe cycle reactions and thus require a long model spin up in order to correctly simulate deep water concentrations. But this would be feasible in a 3-D
20 global OGCBM, since it would only require the addition of two new tracers (L_W and L_S).

5.3 Impact of climate and pH on Fe speciation

While our Fe speciation model has difficulties in reproducing the Fe(II) concentrations measured by Hansard et al. (2009, notwithstanding methodological issues), our model does a good job in the regions we predict to be impacted by climate change and ocean
25 acidification (the high latitudes). It will be necessary to carefully understand the reasons behind the low modeled dFe concentrations in the tropical Pacific as this certainly

BGD

8, 2775–2810, 2011

Towards accounting for dissolved iron speciation

A. Tagliabue and
C. Völker

Title Page

Abstract

Introduction

Conclusions

References

Tables

Figures

⏪

⏩

◀

▶

Back

Close

Full Screen / Esc

Printer-friendly Version

Interactive Discussion



Towards accounting for dissolved iron speciation

A. Tagliabue and
C. Völker

Title Page

Abstract

Introduction

Conclusions

References

Tables

Figures

⏪

⏩

◀

▶

Back

Close

Full Screen / Esc

Printer-friendly Version

Interactive Discussion

restricts the accumulation of Fe(II) therein. Our model suggests that ocean acidification, rather than climate, is likely to exert the strongest control on the evolution of Fe speciation over the coming century through its mediation of redox kinetics. The greater fraction of Fe(II) we simulate agrees with results from mesocosm experiments using natural seawater with bubbled CO₂ (Breitbarth et al., 2010). Laboratory results using synthetic ligands have shown that the complexation of Fe' by ligands could also change with ocean acidification as a function of the degree of protonation of a given ligand, with increases, decreases and no change in complexation possible (Shi et al., 2010). If the in situ ocean ligand pool can be better characterized, and perhaps connected to different production pathways (sensu Hunter and Boyd, 2007), then we could test the combined impact of climate and pH on Fe redox speciation and ligand complexation in the future. Nevertheless, we note that understanding the ultimate impact on the biota will critically depend on the assumptions regarding the nature of the in situ bFe pool.

5.4 Modeling Fe bioavailability

Modeled bFe concentrations are highly sensitive to environmental variability and what Fe species are assumed to be available. In the future, it might be worthwhile to parameterize specific accessibilities of different Fe species to phytoplankton. For example, recent kinetic models (e.g., Völker and Wolf-Gladrow, 1999; Shaked et al., 2005; Salmon et al., 2006; Morel et al., 2008) could be included in our model to more mechanistically treat the bioavailability of the different Fe species we simulate. Or we could assume different accessibilities of strong and weakly complexed Fe to different phytoplankton functional types (Hutchins et al., 1999). The subsequent impact of changes in Fe speciation on primary productivity could then be assessed. In doing so, it would also be important to add more detail to the formulation of the phytoplankton Fe quota (e.g., Flynn, 2003; Buitenhuis and Geider, 2010) so that the impact of environmental changes on the number of photosynthetic units, Fe concentrations, nitrate reductase, as well as different adaptive physiological strategies can also feedback on the phytoplankton demand for Fe (e.g., Raven, 1988; Raven et al., 1999). Assumptions regarding the

availability of specific Fe species could then be tested to explore how the impact of environmental variability on Fe speciation might feedback onto viable phytoplankton Fe uptake strategies.

6 Conclusions

5 Using an analogy with the computation of inorganic carbon speciation in OGCBMs, we outline a means by which Fe speciation can be solved analytically in a cost effective manner in global models. Our approach rests on the division of the Fe cycle into “fast” and “slow” reactions and permits us to simulate 3-D Fe speciation using a global OGCBM. We use our model to show that the distribution of different Fe species is tightly
10 controlled by the dFe concentration, the distribution and concentrations of Fe-binding ligands and environmental variables (temperature, light, oxygen and pH). When compared directly to measurements of Fe(II), our model does a good job of reproducing observations in the high latitude oceans, but systematically underestimates Fe(II) in the low latitude Pacific Ocean (although these may be overestimated). This could result from errors in the modeled dFe field, the absence of the diurnal cycle and high
15 frequency variability, or missing processes from our Fe cycle model (such as Fe(II) binding ligands or specific Fe(II) sources). Using our model under future climate suggests that climate change and, in particular, ocean acidification will impact Fe cycling, especially in the Fe limited Southern Ocean. We predict significant increases in Fe(II) due to acidification, which could reduce the “Fe limited area” of the Southern Ocean by
20 ~ 20% for species that rely solely on assimilating on inorganic Fe. We speculate that a dFe pool that has an increased “free” inorganic component might exert a selective pressure on viable Fe uptake strategies in the future ocean. Finally, our “analytical solution” approach can be used as a framework within which to test our understanding
25 of Fe speciation at the global scale in future studies.

Towards accounting for dissolved iron speciation

A. Tagliabue and
C. Völker

Title Page

Abstract

Introduction

Conclusions

References

Tables

Figures



Back

Close

Full Screen / Esc

Printer-friendly Version

Interactive Discussion



Acknowledgement. The collaboration necessary to initialize this work was formed during two EU COST action (735) workshops in Kiel, Germany, organized by P. Croot. We thank P. Croot and all the participants of these workshops for their input and support. In addition, we specifically thank M. Santana-Casiano and M. González Dávila for providing their oxidation rate equation and help with its implementation, T. Wagener for providing the DOC-ligand equation, K. Barbeau, M. Boye, P. Croot, S. Hansard, and M. Wells for kindly providing published Fe(II) datasets, while G. Sarthou generously provided unpublished Bonus-GoodHope Fe(II) observations and insightful comments on the manuscript, and A. Caubel for assistance with the implementation of the analytical Fe chemistry in NEMO-PISCES. Additional ideas and discussions over the years with K. Arrigo, O. Aumont, A. Bowie, L. Bopp, M. Gehlen, M. Lohan, G. Sarthou, P. Sedwick and Y. Ye were greatly appreciated. A. T. and C. V. acknowledge funding by the “European Project of Ocean Acidification” (EPOCA, grant agreement no. 211384) and “Surface processes in the anthropocene” (SOPRAN, grant agreement 03F0462C), respectively. This work was carried out using HPC resources from GENCI-IDRIS (Grant 2009-10040).



The publication of this article is financed by CNRS-INSU.

References

- Aumont, O. and Bopp, L.: Globalizing results from ocean in situ iron fertilization studies, *Global Biogeochem. Cy.*, 20, GB2017, doi:10.1029/2005GB002591, 2006.
- Aumont, O., Orr, J., Monfray, P., Ludwig, W., Amiotte-Suchet, P., and Probst, J.-L.: Riverine-driven interhemispheric transport of carbon, *Global Biogeochem. Cy.*, 15(02), 393–405, 2001.
- Aumont, O., Bopp, L., and Schulz, M.: What does temporal variability in aeolian dust deposition

BGD

8, 2775–2810, 2011

Towards accounting for dissolved iron speciation

A. Tagliabue and
C. Völker

Title Page

Abstract

Introduction

Conclusions

References

Tables

Figures

⏪

⏩

◀

▶

Back

Close

Full Screen / Esc

Printer-friendly Version

Interactive Discussion



Towards accounting for dissolved iron speciation

A. Tagliabue and
C. Völker

Title Page

Abstract

Introduction

Conclusions

References

Tables

Figures

⏪

⏩

◀

▶

Back

Close

Full Screen / Esc

Printer-friendly Version

Interactive Discussion

contribute to sea-surface iron and chlorophyll distributions?, *Geophys. Res. Lett.*, 35, L07607, doi:10.1029/2007GL031131, 2008.

Barbeau, K., Rue, E. L., Trick, C. G., Bruland, K. W., and Butler, A.: Photochemical reactivity of siderophores produced by marine hetero-trophic bacteria and cyanobacteria based on characteristic Fe(III) binding groups, *Limnol. Oceanogr.*, 48, 1069–1078, 2003.

Boyd, P. W., Jickells, T., Law, C. S., Blain, S., Boyle, E. A., Buesseler, K. O., Coale, K. H., Cullen, J. J., de Baar, H. J., Follows, M., Harvey, M., Lancelot, C., Lepasqueur, M., Owens, N. P., Pollard, R., Rivkin, R. B., Sarmiento, J., Schoemann, V., Smetacek, V., Takeda, S., Tsuda, A., Turner, S., and Watson, A. J.: Mesoscale iron enrichment experiments 1993–2005: synthesis and future directions, *Science*, 315(5812), 612–617, 2007.

Boyd, P. W., Ibsanmi, E., Sander, S. G., Hunter, K. A., and Jackson, G. A.: Remineralization of upper ocean particles: implications for iron biogeochemistry, *Limnol. Oceanogr.*, 55, 1271–1288, 2010.

Breitbarth, E., Gelting, J., Walve, J., Hoffmann, L. J., Turner, D. R., Hassellöv, M., and Ingri, J.: Dissolved iron (II) in the Baltic Sea surface water and implications for cyanobacterial bloom development, *Biogeosciences*, 6, 2397–2420, doi:10.5194/bg-6-2397-2009, 2009.

Breitbarth, E., Bellerby, R. J., Neill, C. C., Ardelan, M. V., Meyerhöfer, M., Zöllner, E., Croot, P. L., and Riebesell, U.: Ocean acidification affects iron speciation during a coastal seawater mesocosm experiment, *Biogeosciences*, 7, 1065–1073, doi:10.5194/bg-7-1065-2010, 2010.

Buck, K. N. and Bruland, K. W.: The physiochemical speciation of dissolved iron in the Bering Sea, Alaska, *Limnol. Oceanogr.*, 52, 1800–1808, 2007.

Buitenhuis, E. T. and Geider, R. J.: A model of phytoplankton acclimation to iron-light colimitation, *Limnol. Oceanogr.*, 55, 714–724, 2010.

Croot, P., Bowie, A., Frew, R., Maldonado, M., Hall, J., Safi, K., LaRoche, J., Boyd, P., and Law, C.: Retention of dissolved iron and FeII in an iron induced Southern Ocean phytoplankton bloom, *Geophys. Res. Lett.*, 28, 3425–3428, 2001.

Croot, P. L., Frew, R. D., Sander, S., Hunter, K. A., Ellwood, M. J., Pickmere, S. E., Abraham, E. R., Law, C. S., Smith, M. J., and Boyd, P. W.: Physical mixing effects on iron biogeochemical cycling: FeCycle experiment, *J.-Geophys. Res.-Oceans*, 112, C06015, doi:10.1029/2006JC003748, 2007.

Croot, P. L., Bluhm, K., Schlosser, C., Streu, P., Breitbarth, E., Frew, R., and Van Ardelan, M.: Regeneration of Fe(II) during EIfEX and SOFeX, *Geophys. Res. Lett.*, 35, L19606, doi:10.1029/2008GL035063, 2008.

**Towards accounting
for dissolved iron
speciation**A. Tagliabue and
C. Völker

[Title Page](#)[Abstract](#)[Introduction](#)[Conclusions](#)[References](#)[Tables](#)[Figures](#)[⏪](#)[⏩](#)[◀](#)[▶](#)[Back](#)[Close](#)[Full Screen / Esc](#)[Printer-friendly Version](#)[Interactive Discussion](#)

Cullen, J. T., Bergquist, B. A., and Moffat, J. W.: Thermodynamic characterization of the partitioning of iron between soluble and colloidal species in the Atlantic Ocean, *Mar. Chem.*, 98, 295–303, doi:10.1016/j.marchem.2005.10.007, 2006.

Flynn, K. J.: Modelling multi-nutrient interactions in phytoplankton; balancing simplicity and realism, *Prog. Oceanogr.*, 56, 249–279, 2003.

Galbraith, E. D., Gnanadesikan, A., Dunne, J. P., and Hiscock, M. R.: Regional impacts of iron-light colimitation in a global biogeochemical model, *Biogeosciences*, 7, 1043–1064, doi:10.5194/bg-7-1043-2010, 2010.

Gledhill, M. and van den Berg, C. M. G.: Determination of the complexation of Fe(III) with natural organic complexing ligands in seawater using cathodic stripping voltammetry, *Mar. Chem.*, 47, 41–54, doi:10.1016/0304-4203(94)90012-4, 1994.

Hansard, S. P., Landing, W. M., Measures, C. I., and Voelker, B. M.: Dissolved iron(II) in the Pacific Ocean: measurements from the PO₂ and P16N CLIVAR/CO₂ repeat hydrography expeditions, *Deep-Sea Res. Pt. I*, 56, 1117–1129, 2009.

Hiemstra, T. and van Riemsdijk, W. H.: Biogeochemical speciation of Fe in ocean water, *Mar. Chem.*, 102, 181–197, doi:10.1016/j.marchem.2006.03.008, 2006.

Hunter, K. A. and Boyd, P. W.: Iron-binding ligands and their role in the ocean biogeochemistry of iron, *Environ. Chem.*, 4, 221–232, 2007.

Hutchins, D. A., Witter, A. E., Butler, A., and Luther III, G. W.: Competition among marine phytoplankton for different chelated iron species, *Nature*, 400, 858–861, doi:10.1038/23680, 1999.

Maldonado, M. T. and Price, N. M.: Reduction and transport of organically bound iron by *Thalassiosira oceanica* (Bacillariophyceae), *J. Phycol.*, 37, 298–309, 2001.

Maldonado, M. T., Allen, A. E., Chong, J. C., Lin, K., Leus, D., Karpenko, N., and Harris, S.: Copper dependent iron transport in coastal and oceanic diatoms, *Limnol. Oceanogr.*, 51, 1729–1743, 2006.

Moore, J. K. and Braucher, O.: Sedimentary and mineral dust sources of dissolved iron to the world ocean, *Biogeosciences*, 5, 631–656, doi:10.5194/bg-5-631-2008, 2008.

Morel, F. M. M., Kustka, A. B., and Shaked, Y.: The role of unchelated Fe in the iron nutrition of phytoplankton, *Limnol., Oceanogr.*, 53(1), 400–404, 2008.

Parekh, P., Follows, M., and Boyle, E.: Modelling the global ocean iron cycle, *Global Biogeochem. Cy.*, 18, GB1002, doi:10.1029/2003GB002061, 2004.

Raven, J. A.: The iron and molybdenum use efficiencies of plant growth with different

Towards accounting for dissolved iron speciation

A. Tagliabue and
C. Völker

Title Page

Abstract

Introduction

Conclusions

References

Tables

Figures

⏪

⏩

◀

▶

Back

Close

Full Screen / Esc

Printer-friendly Version

Interactive Discussion

energy, carbon and nitrogen sources, *New Phytol.*, 109, 279–287, doi:10.1111/j.1469-8137.1988.tb04196.x, 1988.

Raven, J. A., Evans, M. C. W., and Korb, R. E.: The role of trace metals in photosynthetic electron transport in O₂-evolving organisms, *Photosynth. Res.*, 100, 111–150, doi:10.1023/A:1006282714942, 1999.

Rose, A. and Waite, T.: Effect of dissolved natural organic matter on the kinetics of ferrous iron oxygenation in seawater, *Environ. Sci. Technol.*, 37, 4877–4886, 2003.

Rue, E. and Bruland, K.: Complexation of iron(III) by natural organic ligands in the Central North Pacific as determined by a new competitive ligand equilibration/adsorptive cathodic stripping voltammetric method, *Mar. Chem.*, 50, 117–138, 1995.

Salmon, T. P., Rose, A. L., Neilan, B. A., and Waite, T. D.: The FeL model of iron acquisition: nondissociative reduction of ferric complexes in the marine environment, *Limnol. Oceanogr.*, 51, 1744–1754, 2006.

Santana-Casiano, J. M., Gonzalez-Davila, M., and Millero, F. J.: Oxidation of nanomolar levels of Fe(II) with oxygen in natural waters, *Environ. Sci. Technol.*, 39(7), 2073–2079, 2005.

Sarmiento, J. L., Slater, R., Barber, R., Bopp, L., Doney, S. C., Hirst, A. C., Kleypas, J., Matear, R., Mikolajewicz, U., Monfray, P., Soldatov, V., Spall, S. A., and Stouffer, R.: Response of ocean ecosystems to climate warming, *Global Biogeochem. Cy.*, 18, GB3003, doi:10.1029/2003GB002134, 2004.

Sarthou, G., Bucciarelli, E., Chever, F., Arhan, M., and Speich, S.: Labile Fe(II) concentrations in the Atlantic Sector of the Southern Ocean along a transect from subtropical domain to the Weddell Sea Gyre, *Biogeosciences*, in preparation, 2011.

Shaked, Y., Kustka, A. B., and Morel, F. M. M.: A general kinetic model for iron acquisition by eukaryotic phytoplankton, *Limnol. Oceanogr.*, 50, 872–882, 2005.

Shi, D., Xu, Y., Hopkinson, B., and Morel, F. M. M.: Effect of ocean acidification on iron availability to marine phytoplankton, *Science*, 327(5966), 676–679, doi:10.1126/science.1183517, 2010.

Tagliabue, A.: A new global database of dissolved iron measurements, in preparation, 2011.

Tagliabue, A. and Arrigo, K. R.: Processes governing the supply of iron to phytoplankton in stratified seas, *J. Geophys. Res.*, 111, C06019, doi:10.1029/2005JC003363, 2006.

Tagliabue, A., Bopp, L., Aumont, O., and Arrigo, K. R.: Influence of light and temperature on the marine iron cycle: from theoretical to global modeling, *Global Biogeochem. Cy.*, 23, GB2017, doi:10.1029/2008GB003214, 2009.

Towards accounting for dissolved iron speciation

A. Tagliabue and
C. Völker

Title Page

Abstract

Introduction

Conclusions

References

Tables

Figures

◀

▶

◀

▶

Back

Close

Full Screen / Esc

Printer-friendly Version

Interactive Discussion

- Takahashi, T., Sutherland, S. C., Wanninkhof, R., Sweeney, C., Feely, R. A., Chipman, D. W., Hales, B., Friederich, G., Chavez, F., Sabine, C., Watson, A., Bakker, D. C. E., Schuster, U., Metzl, N., Yoshikawa-Inoue, H., Ishii, M., Midorikawa, T., Nojiri, Y., Krtzinger, A., Steinhoff, T., Hoppema, M., Olafsson, J., Arnarson, T. S., Tilbrook, B., Johannessen, T., Olsen, A., Bellerby, R., Wong, C. S., Delille, B., Bates, N. R., and de Baar, H. J. W.: Climatological mean and decadal change in surface ocean $p\text{CO}_2$, and net sea-air CO_2 flux over the global oceans, *Deep-Sea Res. Pt. II*, 56, 554–577, doi:10.1016/j.dsr2.2008.12.009, 2009.
- Van den Berg, C.: Evidence for organic complexation of iron in seawater, *Mar. Chem.*, 50, 139–157, 1995.
- Volker, C., Tagliabue, A., and Ye, Y.: Efficient calculation of iron speciation for use in ocean biogeochemical models, in preparation, 2011.
- Voelker, B. and Sulzberger, B.: Effects of fulvic acid on Fe(II) oxidation by hydrogen peroxide, *Environ. Sci. Technol.*, 30, 1106–1114, 1996.
- Völker, C. and Wolf-Gladrow, D.: Physical limits on iron uptake mediated by siderophores or surface reductases, *Mar. Chem.*, 65, 227–244, 1999.
- Wagener, T., Pulido-Villena, E., and Guieu, C.: Dust iron dissolution in seawater: results from a one-year time-series in the Mediterranean Sea, *Geophys. Res. Lett.*, 35, L16601, doi:10.1029/2008GL034581, 2008.
- Weber, L., Voelker, C., Schartau, M., and Wolf-Gladrow, D. A.: Modeling the speciation and biogeochemistry of iron at the Bermuda Atlantic Time-series Study site, *Global Biogeochem. Cy.*, 19(1), GB1019, doi:10.1029/2004GB002340, 2005.
- Weber, L., Völker, C., Oschlies, A., and Burchard, H.: Iron profiles and speciation of the upper water column at the Bermuda Atlantic Time-series Study site: a model based sensitivity study, *Biogeosciences*, 4, 689–706, doi:10.5194/bg-4-689-2007, 2007.
- Wiley, J. D., Kieber, R. J., Seaton, P. J., and Miller, C.: Rainwater as a source of Fe(II)-stabilizing ligands to seawater, *Limnol. Oceanogr.*, 53, 1678–1684, 2008.
- Witter, A. E., Hutchins, D. A., Butler, A., and Luther III, G. W.: Determination of conditional stability constants and kinetic constants for strong model Fe-binding ligands in seawater, *Mar. Chem.*, 69, 1–17, doi:10.1016/S0304-4203(99)00087-0, 2000.
- Ye, Y., Völker, C., and Wolf-Gladrow, D. A.: A model of Fe speciation and biogeochemistry at the Tropical Eastern North Atlantic Time-Series Observatory site, *Biogeosciences*, 6, 2041–2061, doi:10.5194/bg-6-2041-2009, 2009.

Towards accounting for dissolved iron speciation

A. Tagliabue and
C. Völker

Title Page

Abstract

Introduction

Conclusions

References

Tables

Figures

◀

▶

◀

▶

Back

Close

Full Screen / Esc

Printer-friendly Version

Interactive Discussion

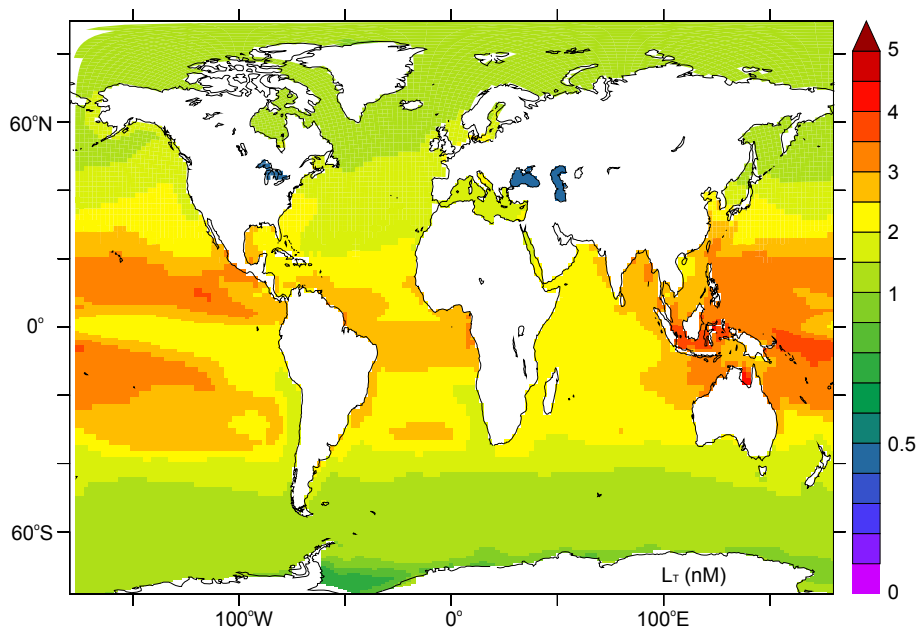


Fig. 1. The distribution of Fe binding ligands when they are computed from an empirical relationship between L_T and DOC (Wagener et al., 2008).

Towards accounting for dissolved iron speciation

A. Tagliabue and
C. Völker

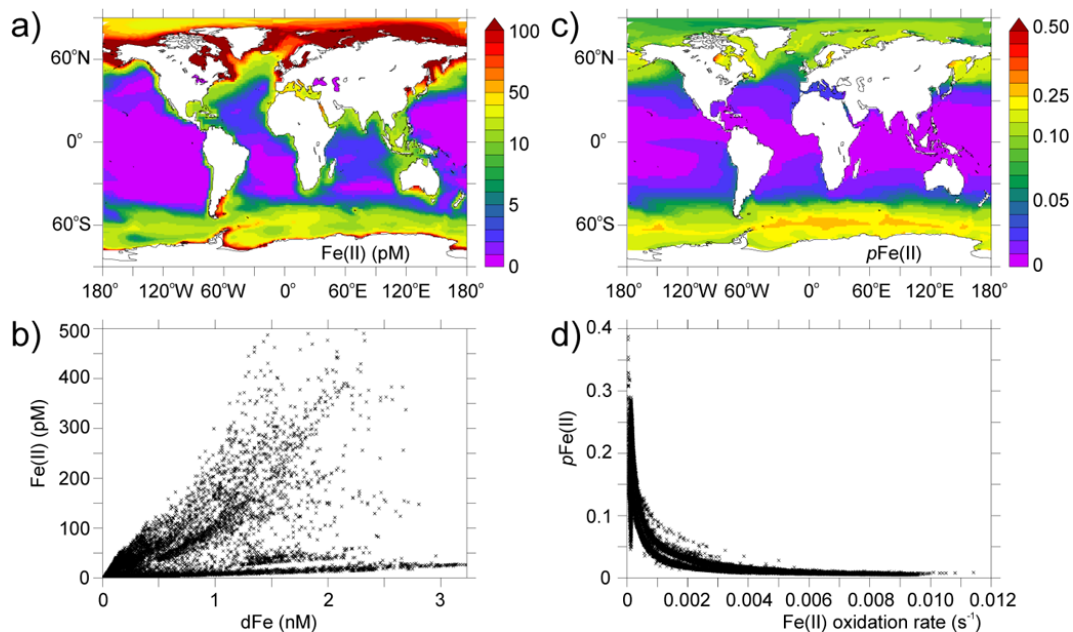


Fig. 2. Annually averaged surface **(a)** dissolved Fe(II) (pM) and **(b)** its relationship to dFe (nM), and **(c)** the annually average surface proportion of the dFe pool present as Fe(II) and **(d)** its relationship to the oxidation rate constant (s^{-1}).

[Title Page](#)[Abstract](#)[Introduction](#)[Conclusions](#)[References](#)[Tables](#)[Figures](#)[◀](#)[▶](#)[◀](#)[▶](#)[Back](#)[Close](#)[Full Screen / Esc](#)[Printer-friendly Version](#)[Interactive Discussion](#)

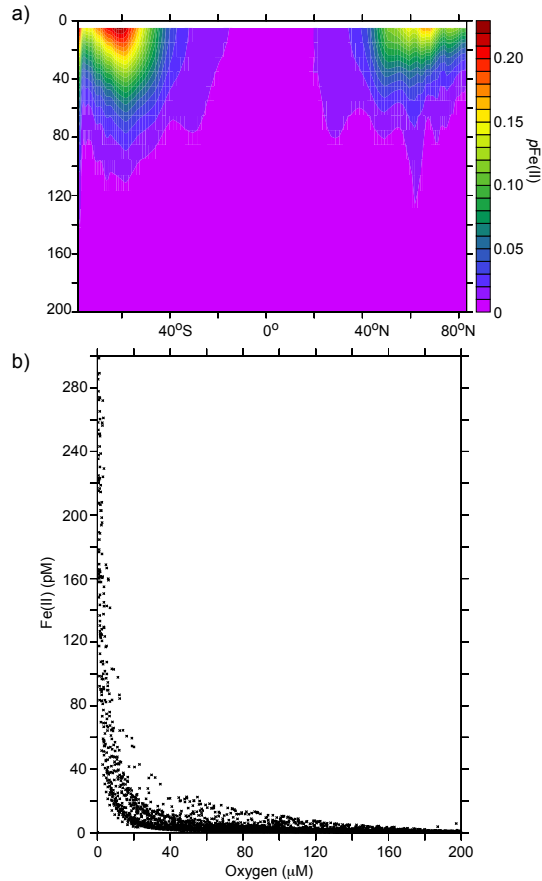


Fig. 3. (a) The zonally averaged pFe(II) for the upper 250 m and (b) the relationship between Fe(II) and oxygen concentration between 200 and 300 m, highlighting the accumulation of Fe(II) in suboxic zones.

Towards accounting for dissolved iron speciation

A. Tagliabue and
C. Völker

Title Page

Abstract

Introduction

Conclusions

References

Tables

Figures



Back

Close

Full Screen / Esc

Printer-friendly Version

Interactive Discussion



Towards accounting for dissolved iron speciation

A. Tagliabue and
C. Völker

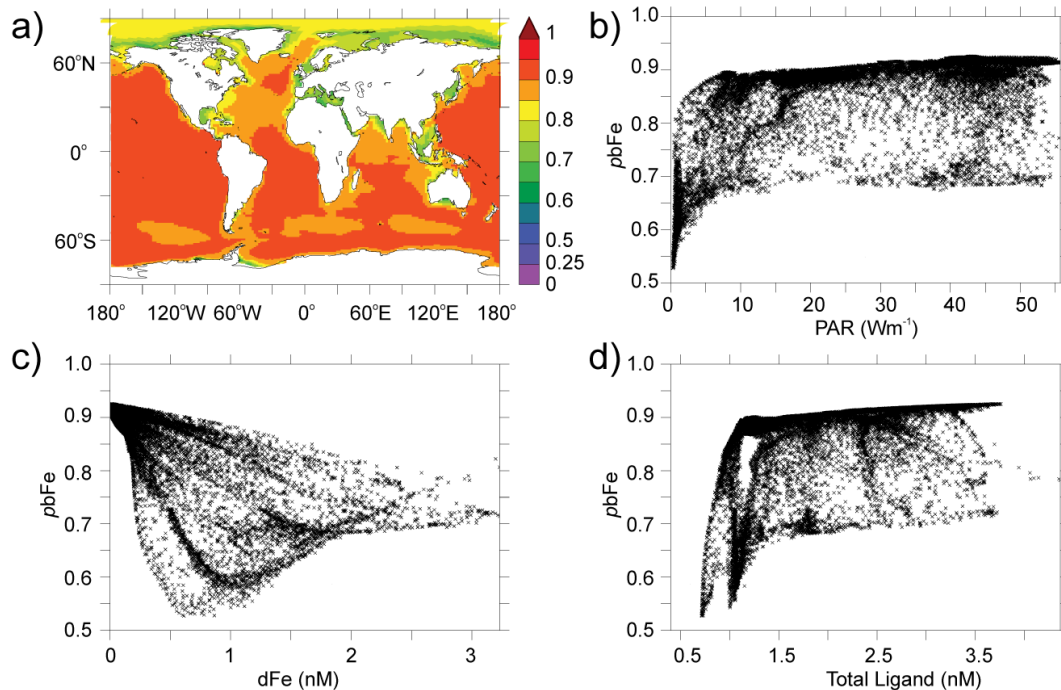


Fig. 4. The (a) annual maximum surface proportion of the dFe pool present as bFe and its relationship to (b) irradiance ($W m^{-2}$), (c) the dFe concentration (nM) and (d) the total concentration of ligands (nM), when bFe is assumed to equal $Fe(II) + Fe(III) + FeL_S$.

Title Page

Abstract

Introduction

Conclusions

References

Tables

Figures

◀

▶

◀

▶

Back

Close

Full Screen / Esc

Printer-friendly Version

Interactive Discussion

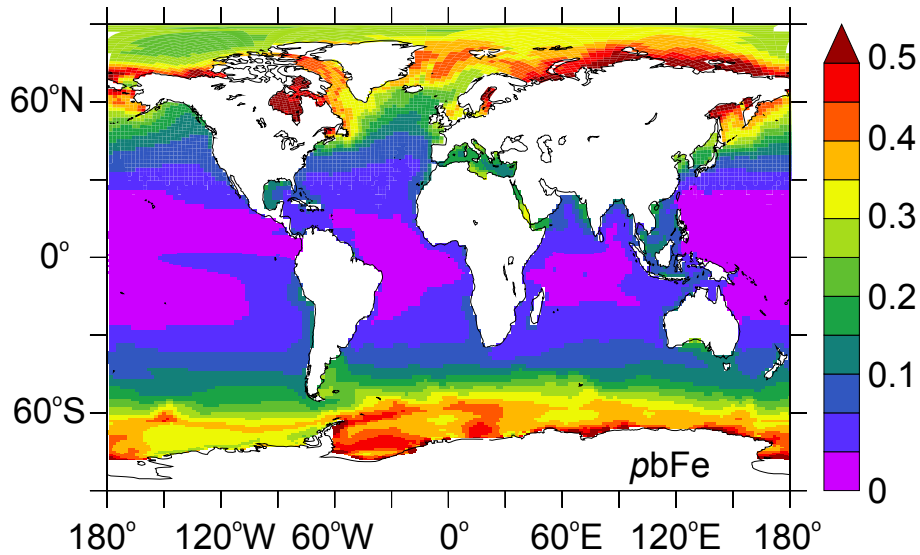


Fig. 5. The annually averaged proportion of the dFe pool present as bFe pool when bFe is assumed to only equal Fe(II) + Fe(III) (compare to Fig. 4a).

Towards accounting for dissolved iron speciation

A. Tagliabue and
C. Völker

Title Page

Abstract Introduction

Conclusions References

Tables Figures

⏪ ⏩

◀ ▶

Back Close

Full Screen / Esc

Printer-friendly Version

Interactive Discussion

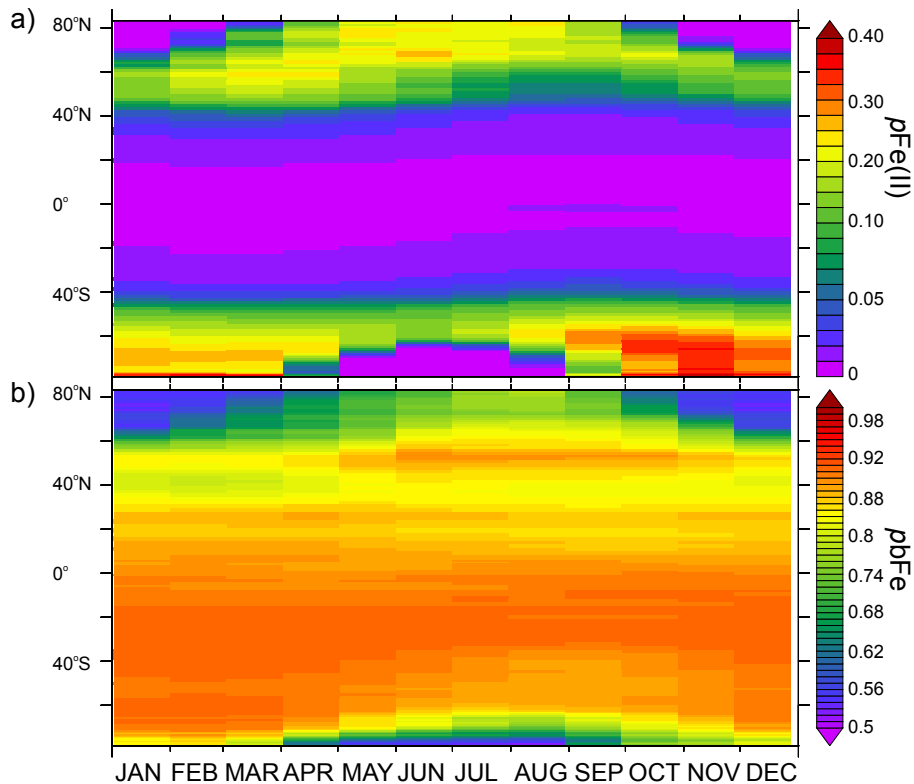


Fig. 6. Seasonal variability in the zonally averaged proportion of the dFe pool present as **(a)** Fe(II) and **(b)** bFe.

Towards accounting for dissolved iron speciation

A. Tagliabue and C. Völker

Title Page

Abstract Introduction

Conclusions References

Tables Figures

◀ ▶

◀ ▶

Back Close

Full Screen / Esc

Printer-friendly Version

Interactive Discussion



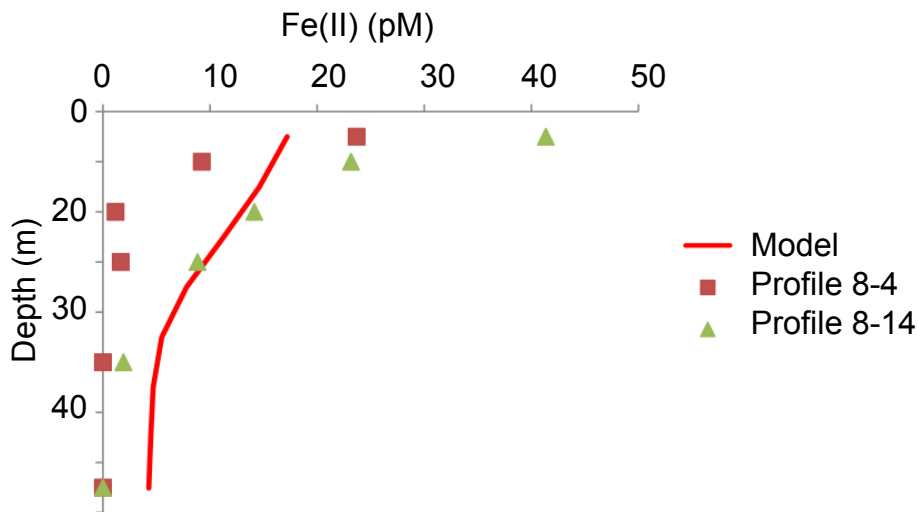


Fig. 7. A profile of modeled Fe(II) alongside profiles 8–4 (47° 35.852' N, 165° 58.760' E) and 8–14 (47° 51.220' N, 166° 15.244' E) presented in Roy et al. (2008).

Towards accounting for dissolved iron speciation

A. Tagliabue and C. Völker

Title Page

Abstract Introduction

Conclusions References

Tables Figures

◀ ▶

◀ ▶

Back Close

Full Screen / Esc

Printer-friendly Version

Interactive Discussion



Towards accounting for dissolved iron speciation

A. Tagliabue and
C. Völker

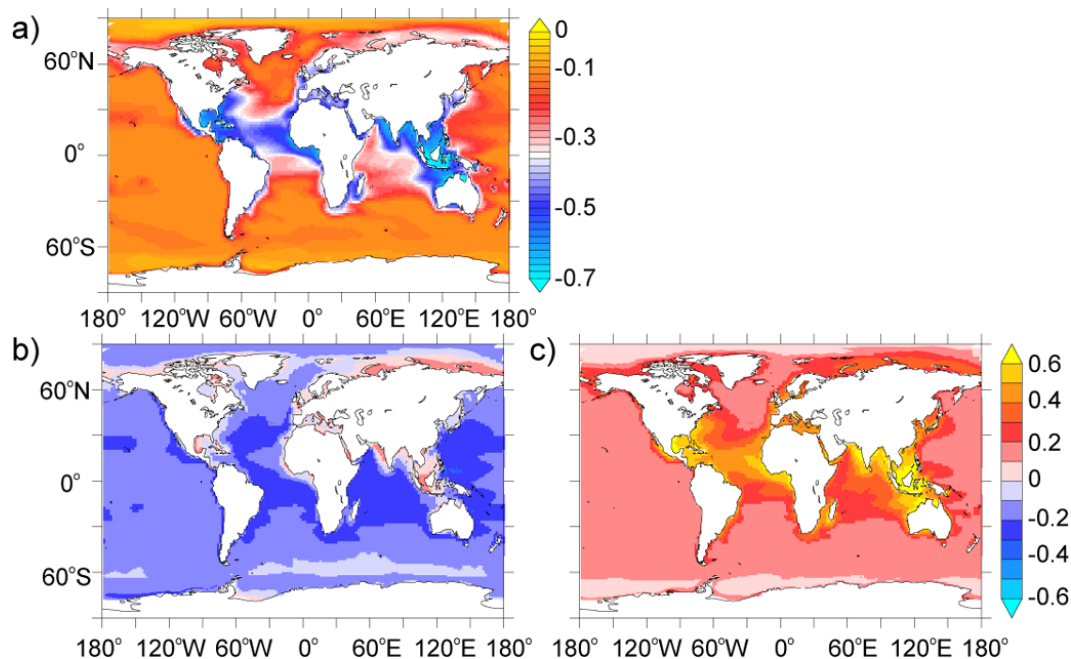


Fig. 8. The proportional change (i.e., $(X_{\text{fixlig}} - X_{\text{varlig}})/X_{\text{varlig}}$) in the proportion of the dFe pool **(a)** organically complexed, **(b)** present as bFe when $\text{bFe} = \text{Fe(II)} + \text{Fe(III)} + \text{FeL}_S$ and **(c)** present as bFe when $\text{bFe} = \text{Fe(II)} + \text{Fe(III)}$ when ligands are assumed to be fixed at 0.6 nM

Title Page

Abstract

Introduction

Conclusions

References

Tables

Figures

◀

▶

◀

▶

Back

Close

Full Screen / Esc

Printer-friendly Version

Interactive Discussion

Towards accounting for dissolved iron speciation

A. Tagliabue and
C. Völker

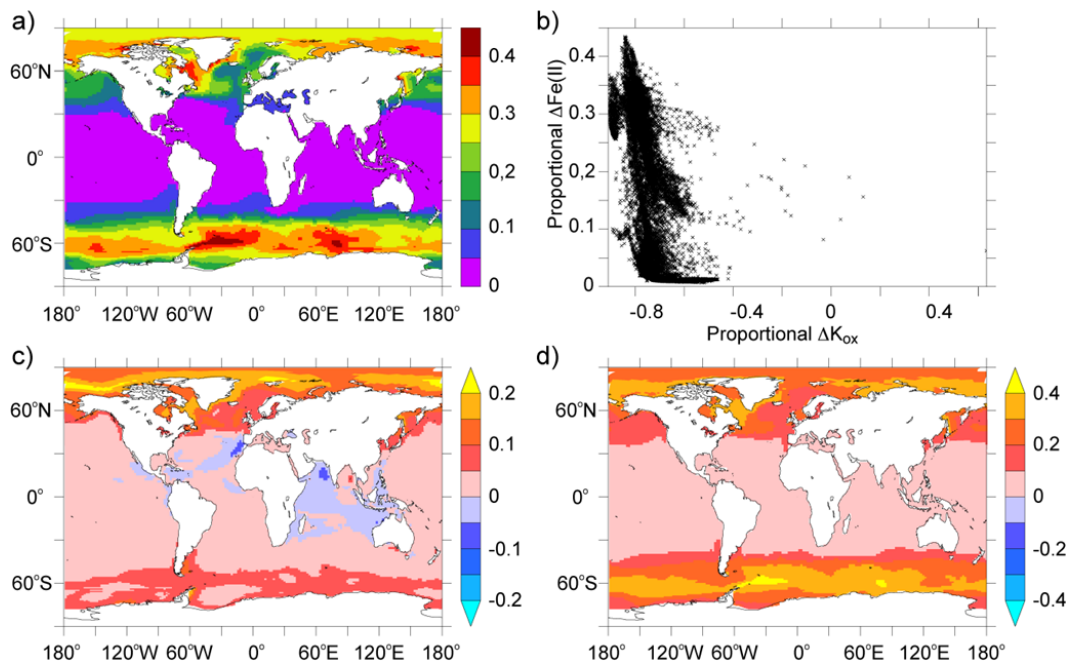


Fig. 9. The proportional (i.e., $(X_{\text{high CO}_2} - X_{\text{low CO}_2})/X_{\text{low CO}_2}$) change in the (a) proportion of the dFe pool present as Fe(II) at an atmospheric CO₂ level of ~1000 ppm and (b) its relationship to the proportional change in the oxidation rate constant, and the proportional change in the proportion of the dFe pool present as bFe pool when bFe equals (c) Fe(II) + Fe(III) + FeL_s and (d) Fe(II) + Fe(III).